

This article was downloaded by:

On: 25 January 2011

Access details: *Access Details: Free Access*

Publisher *Taylor & Francis*

Informa Ltd Registered in England and Wales Registered Number: 1072954 Registered office: Mortimer House, 37-41 Mortimer Street, London W1T 3JH, UK



Separation Science and Technology

Publication details, including instructions for authors and subscription information:

<http://www.informaworld.com/smpp/title~content=t713708471>

Dispersion-Free Solvent Extraction of Thallium(III) in Hollow Fiber Contactors

Tatjana M. Trtić^a; Goran T. Vladisljević^b; Jožef J. Čomor^c

^a LABORATORY OF RADIOISOTOPES, VINČA INSTITUTE OF NUCLEAR SCIENCES, BELGRADE, YUGOSLAVIA ^b INSTITUTE OF FOOD TECHNOLOGY AND BIOCHEMISTRY, FACULTY OF AGRICULTURE, UNIVERSITY OF BELGRADE, BELGRADE-ZEMUN, YUGOSLAVIA ^c LABORATORY OF PHYSICS, VINČA INSTITUTE OF NUCLEAR SCIENCES, BELGRADE, YUGOSLAVIA

Online publication date: 08 July 2000

To cite this Article Trtić, Tatjana M. , Vladisljević, Goran T. and Čomor, Jožef J.(2000) 'Dispersion-Free Solvent Extraction of Thallium(III) in Hollow Fiber Contactors', *Separation Science and Technology*, 35: 10, 1587 — 1601

To link to this Article: DOI: 10.1081/SS-100100242

URL: <http://dx.doi.org/10.1081/SS-100100242>

PLEASE SCROLL DOWN FOR ARTICLE

Full terms and conditions of use: <http://www.informaworld.com/terms-and-conditions-of-access.pdf>

This article may be used for research, teaching and private study purposes. Any substantial or systematic reproduction, re-distribution, re-selling, loan or sub-licensing, systematic supply or distribution in any form to anyone is expressly forbidden.

The publisher does not give any warranty express or implied or make any representation that the contents will be complete or accurate or up to date. The accuracy of any instructions, formulae and drug doses should be independently verified with primary sources. The publisher shall not be liable for any loss, actions, claims, proceedings, demand or costs or damages whatsoever or howsoever caused arising directly or indirectly in connection with or arising out of the use of this material.

Dispersion-Free Solvent Extraction of Thallium(III) in Hollow Fiber Contactors

TATJANA M. TRTIĆ

LABORATORY OF RADIOISOTOPES
VINČA INSTITUTE OF NUCLEAR SCIENCES
P.O. BOX 522, 11001 BELGRADE, YUGOSLAVIA

GORAN T. VLADISAVLJEVIĆ

INSTITUTE OF FOOD TECHNOLOGY AND BIOCHEMISTRY
FACULTY OF AGRICULTURE
UNIVERSITY OF BELGRADE
P.O. BOX 127, 11081 BELGRADE-ZEMUN, YUGOSLAVIA

JOŽEF J. ČOMOR*

LABORATORY OF PHYSICS
VINČA INSTITUTE OF NUCLEAR SCIENCES
P.O. BOX 522, 11001 BELGRADE, YUGOSLAVIA

ABSTRACT

Dispersion-free extraction of thallium(III) from $\text{NaCl}/\text{H}_2\text{SO}_4$ solution into butyl acetate has been studied using hydrophobic polypropylene and polyvinylidene fluoride hollow fibers of different effective lengths. The aqueous feed solution flowed inside the fibers and the organic phase was fed at the shell side. The influence of phase flow rates on the mass transfer coefficients was investigated, and correlations between the Sherwood and Graetz numbers were developed. The overall resistance to mass transfer is controlled by the feed-side mass transfer coefficient due to the high partition coefficient of HTlCl_4 between the phases. The obtained results are discussed in terms of extraction efficiency, thallium flux through the interfacial area, and the length of the transfer unit as a function of the feed flow rate and the effective fiber length. The extraction efficiency was independent of the organic phase flow rate.

Key Words. Thallium; Solvent extraction; Hollow fiber; Production of radiopharmaceuticals; $^{201}\text{TlCl}$

* To whom correspondence should be addressed. Telephone: +381-11-444-77-00. FAX: +381-11-444-79-63. E-mail: jcomor@rt270.vin.bg.ac.yu

INTRODUCTION

$^{201}\text{TlCl}$ is a well-known cyclotron-produced radiopharmaceutical for myocardial and tumor imaging (1, 2). The radioisotope ^{201}Tl , required for the production of the radiopharmaceutical, is usually produced by the nuclear reaction $^{203}\text{Tl}(\text{p}, 3\text{n})^{201}\text{Pb} \rightarrow ^{201}\text{Tl}$, followed by subsequent target processing. The key step in the production of $^{201}\text{TlCl}$ is the separation of trace amounts of ^{201}Pb (the parent of ^{201}Tl) from the irradiated target material, metallic ^{203}Tl .

Various radiochemical separation methods, such as precipitation, coprecipitation, ion-exchange chromatography, solvent extraction, and a combination of these methods, can be used for this purpose (3–16). One of the most suitable techniques for the separation of thallium from lead is solvent extraction using butyl acetate (BuAc). The distribution coefficient of Tl(III) between butyl acetate and aqueous phase is about 1000 when the extraction is carried out from 5 $\text{mol}\cdot\text{dm}^{-3}$ H_2SO_4 solution containing NaCl , providing the molar ratios between Tl(III) and Cl^- are not less than 1:4. Tl(III) will be extracted from this solution in the form of a HTlCl_4 complex (17).

A membrane-based solvent extraction using microporous hollow fibers was recently shown to be an effective alternative to conventional dispersion-based solvent extraction. The advantages of membrane-based extractors over conventional devices, such as packed towers, spray towers, etc., are much larger interfacial areas per unit contactor volume; independent control of phase flow rates without loading, flooding, and emulsification problems (18–20); low hold-up volume to avoid the accidental release of radioactive materials; and a good opportunity for process automatization.

A microporous membrane can be hydrophobic or hydrophilic. Hydrophobic membranes are preferable when the main resistance to solute mass transfer is situated in the aqueous phase, which is the case in the present experimental system. Maximization of the overall mass transfer rate is of intrinsic interest in membrane-based solvent extraction as well as in contained liquid membrane permeation where the two-phase interfaces are immobilized as opposed to just one interface in membrane-based solvent extraction (21, 22).

The purpose of this study was to apply this novel membrane extraction method to the separation of Tl(III) from Pb(II) . The extraction of Tl(III) from $\text{NaCl}/\text{H}_2\text{SO}_4$ solution using butyl acetate as an extractant was performed in membrane modules with hydrophobic hollow fibers made of polypropylene (PP) and polyvinylidene fluoride (PVDF).

EXPERIMENTAL

Chemicals and Materials

All experiments were performed with aqueous phases initially containing 0.03 $\text{mol}\cdot\text{dm}^{-3}$ Tl_2SO_4 (Fluka, p.a. grade), 5.0 $\text{mol}\cdot\text{dm}^{-3}$ H_2SO_4 (Merck, p.a.

© Marcel Dekker, Inc. All rights reserved.
270 Madison Avenue, New York, New York 10016



grade), and $0.3 \text{ mol} \cdot \text{dm}^{-3}$ NaCl (Merck, p.a. grade). Trivalent thallium, which is appropriate for extraction with butyl acetate (Fluka, p.a. grade), was obtained by oxidation with excess of KBrO_3 (Merck, p.a. grade). The concentration of Tl(III) in the aqueous and organic phases was determined by labeling the initial feed solution with $^{201}\text{TlCl}$ (CIS bio international) followed by subsequent determination of the activities of both phases using an automated γ -counter (LKB WalLac, CompuGama Model 1282-001) (17).

Experimental Setup and Procedures

Four microporous hollow-fiber modules were constructed and used in this study. The modules were made by placing the specified number of hydrophobic polypropylene (Celgrad X-20) or polyvinylidene fluoride (Akzo Enka) fibers into an external glass shell with an inner diameter of 1 cm. The fibers were potted on both ends of the shell with epoxy resin. The main characteristics of contactors and hollow fibers are given in Table 1.

The membrane-based solvent extraction system, shown in Fig. 1, consisted of a hollow-fiber module; four reservoirs of 100 cm^3 for the feed solution (R1), rafinate (R2), solvent (R3), and extract (R4); two peristaltic pumps; and tubes. All experiments were carried out at a constant temperature of 291 K.

The feed solution was pumped from reservoir R1 by a Perkin-Elmer peristaltic pump at a flow rate of $0.65\text{--}10 \text{ cm}^3 \cdot \text{min}^{-1}$. The feed solution flowed continuously through the fibers in an once-through mode, and the rafinate was collected in reservoir R2. It is known that a significant portion of the shell-side fluid may flow along the outside of the tube bundle, and not within the tube

TABLE 1
Characteristics of Hollow Fiber Modules

| | Module no. | | | |
|--|------------|-------|-------|-------|
| | 1 | 2 | 3 | 4 |
| Membrane polymer | PVDF | PVDF | PP | PP |
| Length of module (m) | 0.103 | 0.14 | 0.09 | 0.14 |
| No. of fibers in a module, N | 31 | 30 | 30 | 31 |
| Effective fiber length, L (m) | 0.068 | 0.122 | 0.065 | 0.120 |
| Inner fiber diameter, d_i (μm) ^a | 254 | 254 | 280 | 280 |
| Outer fiber diameter, d_o (μm) ^a | 648 | 648 | 660 | 660 |
| Membrane wall porosity, ε (%) ^b | 35 | 35 | 28 | 28 |

^a Diameters of hollow fibers, previously saturated with butyl acetate, were determined under a microscope (Zeiss, FRG) using polarized light.

^b The porosity of the membrane wall was experimentally determined using a procedure suggested by Prasad and Sirkar (25).



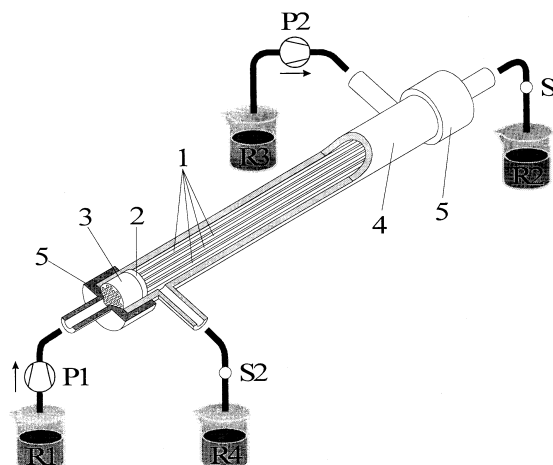


FIG. 1 Schematic of the experimental setup showing a section through the contactor housing: (1) hollow fibers, (2) punched Teflon disk ensuring the fiber geometry, (3) epoxy resin, (4) glass housing, (5) end connectors, (P1–P2) peristaltic pumps, (S1–S2) sample ports, (R1–R4) reservoirs.

bundle (23, 24). Seibert et al. (23) showed that the actual residence time of the shell-side fluid in a commercial unbaffled hollow fiber extractor was 3–4 times shorter than the ideal residence time, and as a result only 10–30% of the membrane surface area was effective for mass transfer. In order to avoid the detrimental effect of shell-side bypassing on the mass transfer performance of our contactors, the feed solution was always sent through the tube-side. In addition, the small number of fibers in the contactor (30 and 31 only) and appropriately punched Teflon disks at both ends of the module (see Fig. 1) ensured that the fibers were not touching each other. The organic phase was pumped countercurrently at the shell-side of the module at a flow rate of $1.1 \text{ cm}^3 \cdot \text{min}^{-1}$. Since the fibers are hydrophobic, the pores of the membrane were filled with organic solution. The aqueous phase pressure was maintained higher than the organic phase pressure to prevent leakage of the organic phase from the pores into the aqueous phase. In order to determine the Tl(III) concentration, samples of 0.5 cm^3 were taken at the outlet of the aqueous and organic phases in regular time intervals of 2 minutes until a steady state was established.

The steady-state Tl(III) concentrations were used to calculate the overall mass transfer coefficient K_w based on aqueous phase according to the following equation:

$$K_w = \frac{Q_w}{\pi d_i N L} \ln \left(\frac{C_w^{\text{in}}}{C_w^{\text{out}}} \right) \quad (1)$$

where the various symbols are defined in the Symbols section. Equation (1) is the simplified form of the general solution (25) which is valid for high solute



distribution coefficients ($m_i \gg 1$). In our case the distribution coefficient m_i , defined as the equilibrium concentration of HTlCl_4 in the organic phase (butyl acetate) divided by that in the aqueous phase (5 $\text{mol}\cdot\text{dm}^{-3}$ H_2SO_4 and 1 $\text{mol}\cdot\text{dm}^{-3}$ NaCl), was found to be 1180 at 291 K (17). It must be noted here that the overall mass transfer resistance for thallium transfer is given by

$$\frac{1}{K_w} = \frac{1}{k_w} + \frac{d_i}{m_i d_{lm} k_{mo}} + \frac{d_i}{m_i d_o k_o} \quad (2)$$

RESULTS AND DISCUSSION

A typical time variation of Tl(III) concentration in the aqueous phase at the outlet of the module, C_w^{out} , is given in Fig. 2. The steady state was typically established within 4–6 and 8–10 minutes for the shorter and longer modules, respectively. These time intervals are comparable to those observed in conventional dispersion-phase extraction of Tl(III) using the same extractant (17), and they were independent on the membrane material used. The time in which the stationary state is attained in our modules is very short in comparison with the 50 minutes found by Giorno et al. (26) for the membrane-based solvent extraction of lactic acid from fermentation broths with Aliquat 336 and the 120 minutes observed by Kim et al. (27) for membrane-based extraction of Cu(II) with β -hydroxyoxime. This discrepancy is due to the rather high distribution coefficient of Tl(III) compared to the above mentioned systems.

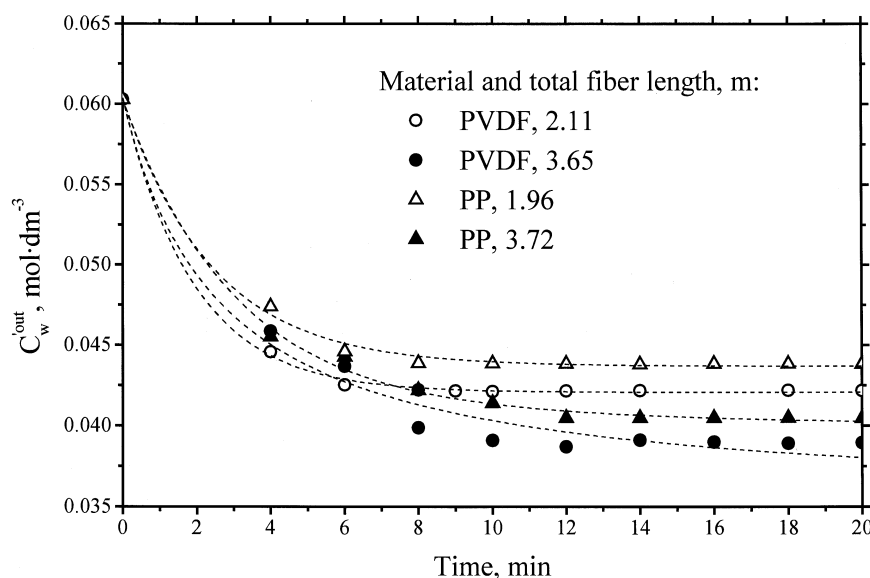


FIG. 2 Concentration profile of Tl(III) in the outlet of feed as a function of total fiber length and membrane materials used. The aqueous flow rate was $1.8 \text{ cm}^3 \cdot \text{min}^{-1}$, and the organic flow rate was $1.1 \text{ cm}^3 \cdot \text{min}^{-1}$.



The steady-state outlet concentrations of Tl(III) in the aqueous phase, C_w^{out} , as a function of aqueous phase flow rate, Q_w , is shown in Fig. 3. One can see that C_w^{out} increases either by increasing Q_w or by decreasing the module length. The same type of behavior was reported by Guha et al. (28) for the removal of heavy metals from wastewater by hollow fibers contained in a liquid membrane permeator.

Figure 4 shows the dependence of the overall mass transfer coefficient, K_w , on the organic phase flow rate, Q_o , at a constant feed flow rate of $1.8 \text{ cm}^3 \cdot \text{min}^{-1}$. Obviously, the organic phase flow rate has no influence on the mass transfer rate, which can be explained by a very high value of m_i . Thus, in the subsequent experiments the organic phase flow rate was maintained constant ($1.1 \text{ cm}^3 \cdot \text{min}^{-1}$).

Figure 5 is a plot of the overall mass transfer coefficient, K_w , vs the aqueous flow rate, Q_w , on a log-log scale. A linear dependence was obtained, indicating that the overall mass-transfer resistance is controlled by the aqueous phase resistance, so that $K_w \approx k_w$. The same type of linear dependence for systems of $m_i \gg 1$ was reported for the removal of heavy metals from wastewater (28), the extraction of the pharmaceutical product diltiazem with decyl alcohol (29), and the backextraction of phenol (21). On the other hand, a nonlinear dependence for a system of $m \gg 1$ was observed for the solvent extraction of citric acid with tri-*n*-octylamine (30).

At the same Q_w value and membrane type, K_w decreases with increasing L , which is in agreement with the laminar flow correlation developed by Lévéque (31), Sieder and Tate (32), and Dahuron and Cussler (33). In our experiments

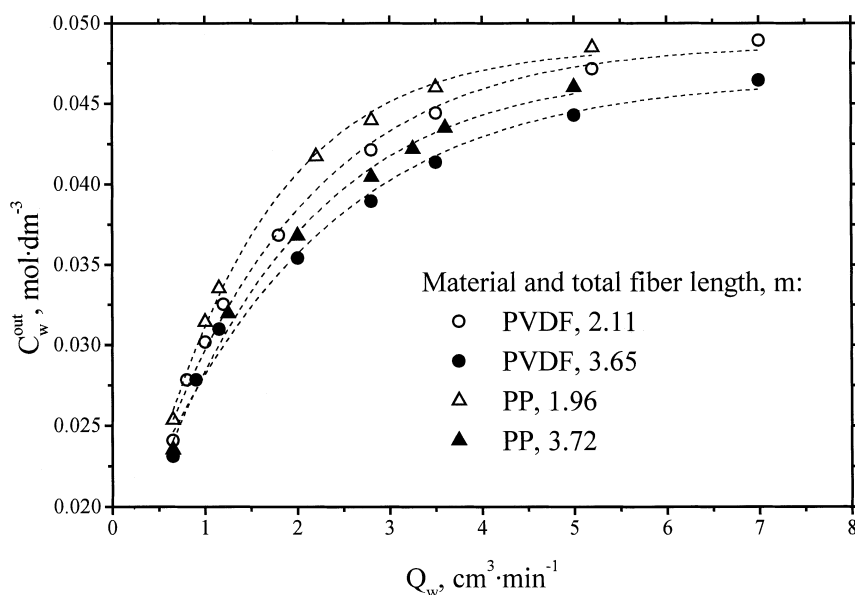


FIG. 3 Effect of the feed flow rate variation on the outlet Tl(III) concentration in the feed stream.



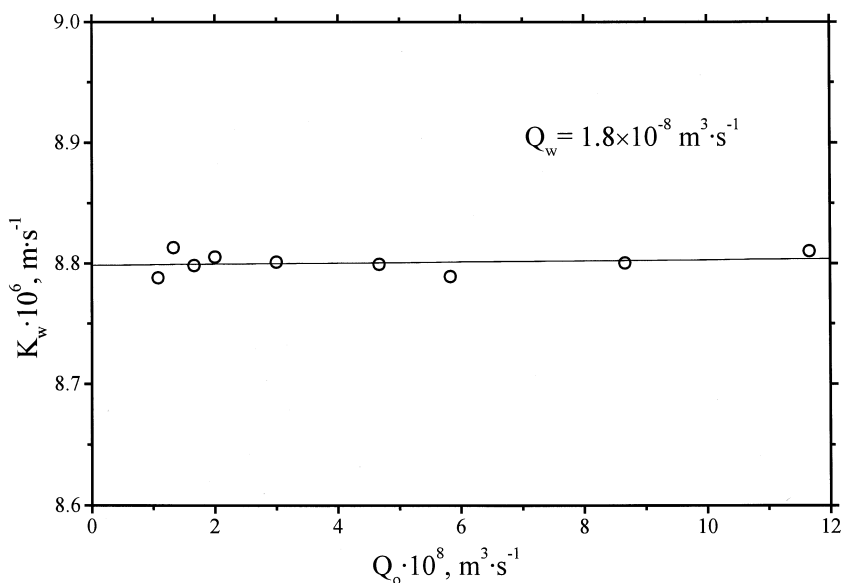


FIG. 4 Effect of the organic flow variation on the overall mass transfer coefficient of Tl(III) based on the aqueous phase, in a PVDF contactor with 2.11 m total fiber length. The feed flow rate was kept constant at $1.1 \text{ cm}^3 \cdot \text{min}^{-1}$.

the Reynolds number in the aqueous phase flow was in the 10–125 range, which is an indication of a laminar regime (34). The membrane polymer plays no important role in the thallium(III) permeation rate since the membrane resistance is negligible. Namely, the membrane mass-transfer coefficient k_{mo} de-

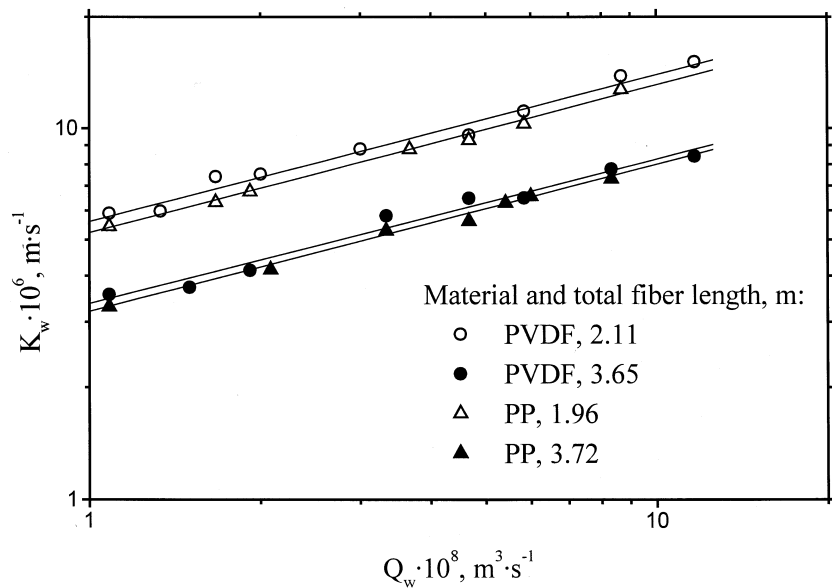


FIG. 5 Effect of the aqueous flow rate on the overall mass transfer coefficient of Tl(III) based on the aqueous phase. The organic flow rate was kept constant ($1.1 \text{ cm}^3 \cdot \text{min}^{-1}$). The solid lines represent predicted K_w calculated by Eqs. (3)–(6).

MARCEL DEKKER, INC.
270 Madison Avenue, New York, New York 10016



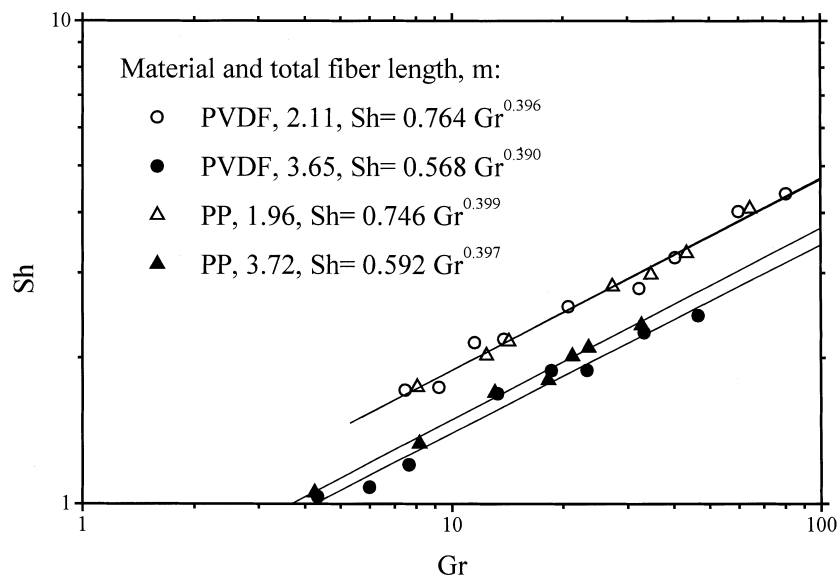


FIG. 6 Tube-side Sherwood number, Sh, as a function of Graetz number, Gr. The solid lines represent Sh values calculated from analytical K_w expressions (Eqs. 3–6).

pends on the porosity ε , thickness δ , and tortuosity τ of the hollow fiber wall according to: $k_{mo} = D_o \varepsilon / (\delta \tau)$, where $D_o = 1.65 \times 10^{-9} \text{ m}^2 \cdot \text{s}^{-1}$ is the HTlCl_4 diffusivity in butyl acetate at 291 K calculated from the Wilke–Chang correlation (35). For PP fibers, $\varepsilon = 0.28$, $\delta = 1.9 \times 10^{-4} \text{ m}$, and $\tau = 2.5$ according to Prasad and Sirkar (25), from which one obtains $k_{mo} = 9.72 \times 10^{-7} \text{ m} \cdot \text{s}^{-1}$. The substitution of this k_{mo} value into the second right-hand term of Eq. (2) gives a membrane resistance value of around $550 \text{ s} \cdot \text{m}^{-1}$. This is more than two orders of magnitude lower than $7.9 \times 10^4 \text{ s} \cdot \text{m}^{-1}$, which is the minimum value of the overall mass-transfer resistance $1/K_w$ for the data in Fig. 5.

A least-square regression of the data in Fig. 5 gave the following correlation:

$$\text{PVDF, } NL = 2.11 \text{ m: } K_w = 8.248 \times 10^{-3} Q_w^{0.396} \quad (3)$$

$$\text{PVDF, } NL = 3.65 \text{ m: } K_w = 4.433 \times 10^{-3} Q_w^{0.390} \quad (4)$$

$$\text{PP, } NL = 3.72 \text{ m: } K_w = 4.806 \times 10^{-3} Q_w^{0.397} \quad (5)$$

$$\text{PP, } NL = 1.96 \text{ m: } K_w = 8.130 \times 10^{-3} Q_w^{0.399} \quad (6)$$

The correlation coefficients exceeded 0.99 in all cases. In Fig. 6 the K_w values expressed in terms of the Sherwood number, Sh, were plotted against the aqueous phase flow rate in terms of the Graetz number, Gr. The Sherwood number for aqueous flow on the tube-side can be expressed as

$$Sh = K_w d_i / D \quad (7)$$



where $D = 8.74 \times 10^{-10} \text{ m}^2 \cdot \text{s}^{-1}$ is the HTlCl_4 diffusivity in the aqueous phase at 291 K as calculated from the Wilke-Chang correlation (35). The Graetz number was calculated using the following equation:

$$\text{Gr} = \text{ReSc} \frac{d_i}{L} = \frac{4Q_w}{\pi d_i N \nu} \frac{\nu}{D} \frac{d_i}{L} = \frac{4Q_w}{\pi N L D} \quad (8)$$

The linear dependence obtained is similar to the results described by Yang and Cussler (36) for bubbleless water deoxygenation and carbonation, and by Prasad and Sirkar (37) for the nondispersive solvent extraction of 4-methylthiazole and 4-cyanothiazole with toluene and benzene. The exponent on Gr in the mass transfer correlation given in Fig. 6 ranges between 0.390 and 0.399, which is higher than the 0.33 anticipated in the Lévêque equation (31) but lower than the 0.5 predicted by the Gröber equation (38). Lévêque's solution is applicable in the 100–5000 Gr range, and the correlation presented by Gröber et al. (38) holds for the special case in which the velocity profile develops down the full fiber length. In our experiments Gr varied between 4.2 and 81 and the entry length was in the 0.08–0.13 cm range, which is much lower than the fiber length. Therefore, neither the Lévêque nor the Gröber correlation strictly applies for our experimental conditions.

Wilson plots of $1/K_w$ vs Q_w^{-b} are shown in Fig. 7. The values of the exponent, b , were determined by a least-square fit of K_w vs Q_w (Eqs. 3–6). As expected, the intercept on the $1/K_w$ axis is equal to zero, indicating that the ma-

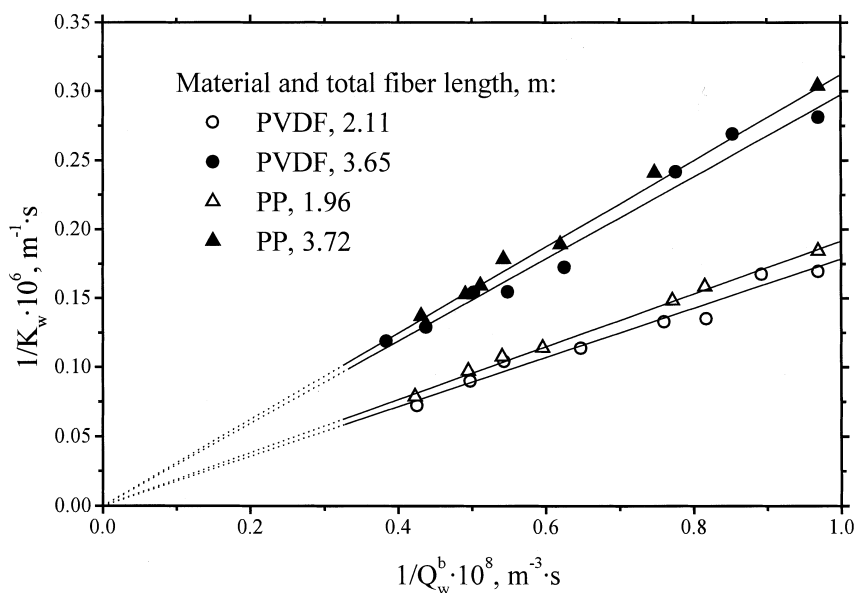


FIG. 7 Wilson plot of $1/K_w$ vs Q_w^{-b} , where b is a coefficient from Eqs. (3)–(6). The solid lines represent predicted K_w calculated by Eqs. (3)–(6).



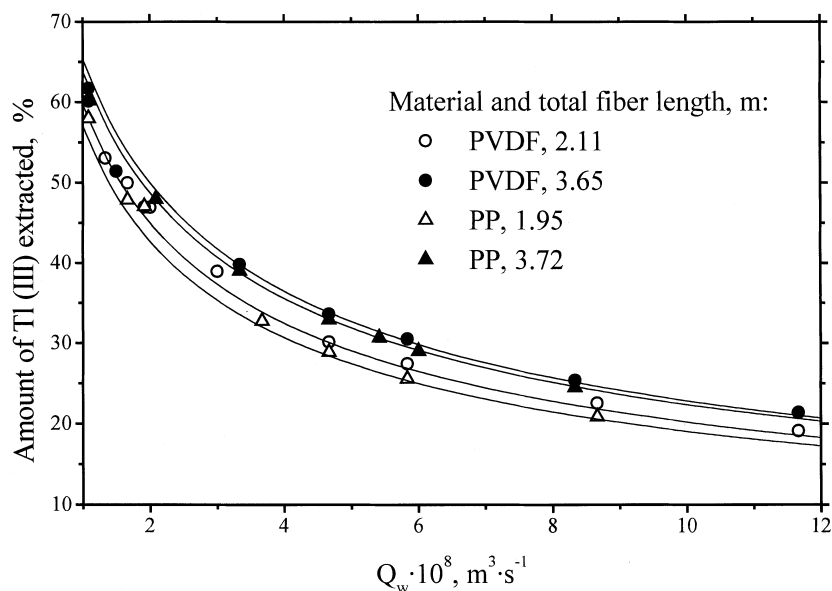


FIG. 8 The percent of Tl(III) extracted as a function of the aqueous flow rate. The solid lines represent predicted E values calculated by Eqs. (11)–(14).

major mass-transfer resistance for Tl(III) transfer is in the aqueous phase (25, 37, 39, 40).

Figure 8 shows the amount of Tl(III) extracted from the aqueous feed stream to the organic stream at different feed flow rates. The extraction extent of thallium(III) can be expressed as

$$E = \frac{C_w^{\text{in}} - C_w^{\text{out}}}{C_w^{\text{in}}} = 1 - \frac{C_w^{\text{out}}}{C_w^{\text{in}}} \quad (9)$$

From Eqs. (1) and (9) the extraction extent of Tl(III) is given by

$$E = 1 - \exp\left(-\frac{K_w L \pi d_i}{Q_w}\right) \quad (10)$$

Substituting Eqs. (3)–(6) into Eq. (10), one obtains the relations between E and Q_w :

$$\text{PVDF, } NL = 2.11 \text{ m: } E = 1 - \exp(-1.336 \times 10^{-5} Q_w^{-0.604}) \quad (11)$$

$$\text{PVDF, } NL = 3.65 \text{ m: } E = 1 - \exp(-1.392 \times 10^{-5} Q_w^{-0.610}) \quad (12)$$

$$\text{PP, } NL = 3.72 \text{ m: } E = 1 - \exp(-1.520 \times 10^{-5} Q_w^{-0.603}) \quad (13)$$

$$\text{PP, } NL = 1.96 \text{ m: } E = 1 - \exp(-1.312 \times 10^{-5} Q_w^{-0.601}) \quad (14)$$

It can be seen that E decreases with increasing Q_w and with decreasing the module length in the 18–65% range. As the aqueous phase flow rate increases, the residence time of the aqueous phase in the contactor decreases, allowing

less time for mass transfer to occur, and therefore the amount of Tl(III) extracted decreases. The same type of behavior was obtained by Basu and Sirkar (29) for the extraction of diltiazem with decyl alcohol (30–90%), Prasad and Sirkar (37) for the dispersion-free solvent extraction of 4-methylthiazole and 4-cyanothiazole with toluene and benzene (20–60%), Seibert and Fair (41) for the extraction of hexanol from water with octanol (20–45%), and Knutsson et al. (42) for the extraction of pesticides with a mixture of *n*-undecane and di-*n*-hexyl ether (15–60%).

The effective length L of a single fiber can be expressed as

$$L = \text{NTU} \times \text{LTU} = \frac{C_w^{\text{in}} - C_w^{\text{out}}}{\Delta C_{\text{lm}}} \frac{Q_w}{K_w \pi d_u N} = \ln\left(\frac{C_w^{\text{in}}}{C_w^{\text{out}}}\right) \frac{Q_w}{K_w \pi d_i N} \quad (15)$$

High values of LTU show poorly contacted phases (25). Substituting Eqs. (3)–(6) into Eq. (15), one obtains the relations between the length of transfer unit LTU and Q_w :

$$\text{PVDF, } NL = 2.11 \text{ m:} \quad \text{LTU} = 4.904 \times 10^3 Q_w^{0.604} \quad (16)$$

$$\text{PVDF, } NL = 3.65 \text{ m:} \quad \text{LTU} = 9.266 \times 10^3 Q_w^{0.610} \quad (17)$$

$$\text{PP, } NL = 3.72 \text{ m:} \quad \text{LTU} = 7.630 \times 10^3 Q_w^{0.603} \quad (18)$$

$$\text{PP, } NL = 1.96 \text{ m:} \quad \text{LTU} = 4.510 \times 10^3 Q_w^{0.601} \quad (19)$$

Figure 9 shows LTU as a function of Q_w and NL . It is clear that the experimental LTU values are in good agreement with the calculated LTU values rep-

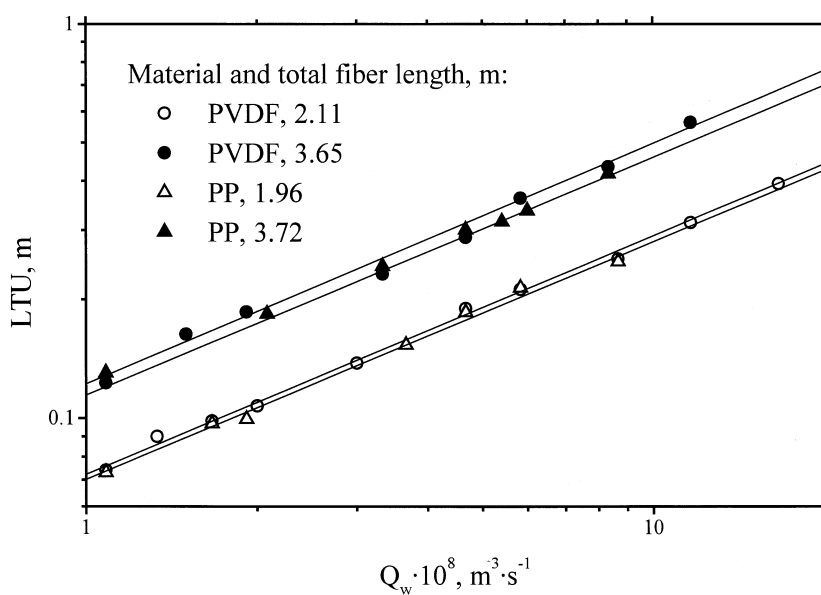


FIG. 9 The length of the transfer unit, LTU, versus the aqueous flow rate. The solid lines represent predicted LTU calculated by Eqs. (16)–(19).

MARCEL DEKKER, INC.
270 Madison Avenue, New York, New York 10016



resented by the solid lines. As the aqueous phase flow rate and the total fiber length decrease, LTU decreases. This can be explained by the fact that NTU increases with decreasing Q_w due to a decrease in both C_w^{out} and ΔC_{lm} . Such LTU dependencies on Q_w are also reported by Prasad and Sirkar (25) for the dispersion-free solvent extraction of various solutes, and by Keurentjes et al. (43) for the separation of racemic mixtures. It must be noted from Fig. 9 that LTU values as low as 6 cm were achieved in shorter modules, which is an order of magnitude lower than the lowest LTU values reported in conventional dispersion-based contactors (25).

The mean flux \bar{J} of Tl(III) through the interfacial area A is given by

$$\bar{J} = \frac{1}{A} \int_0^A J dA = \frac{Q_w}{\pi d_i N L} (C_w^{\text{in}} - C_w^{\text{out}}) = K_w \Delta C_{\text{lm}} \quad (20)$$

where J is the local flux of Tl(III). In Fig. 10 the mean flux of Tl(III) is plotted against the aqueous phase flow rate. The thallium(III) flux through the interfacial area increases with increasing aqueous phase flow rate due to an increase in both ΔC_{lm} and K_w . At the same aqueous phase flow rate, the thallium(III) flux is higher for the shorter modules since K_w is higher at lower L values. However, the physical properties of the membrane wall do not influence the Tl(III) flux. Similar relations between J and Q_w are also reported elsewhere (21, 27). At sufficiently high phase flow rates, the thallium(III) flux is limited by the membrane resistance and the inlet Tl(III) concentration in the

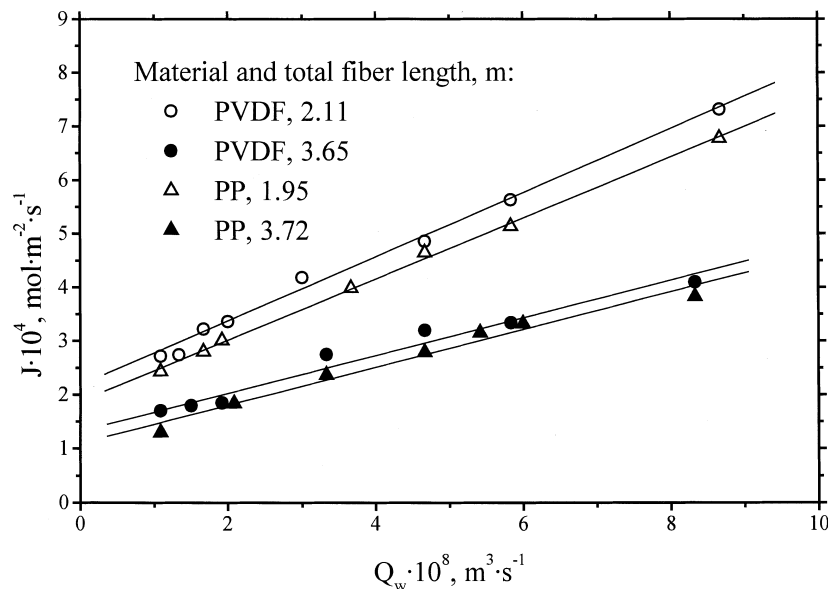


FIG. 10 The variation of the mean Tl(III) flux through the interfacial area with the aqueous feed flow rate and module length.



feed stream. If the inlet Tl(III) concentration in the aqueous feed is $0.06 \text{ mol}\cdot\text{dm}^{-3}$ as in Fig. 10, the limiting Tl(III) flux is around $0.1 \text{ mol}\cdot\text{m}^{-2}\cdot\text{s}^{-1}$, which is 2–3 orders of magnitude higher than the mean Tl(III) fluxes reported in Fig. 10.

CONCLUSION

The applicability of dispersion-free solvent extraction of thallium with butyl acetate in hollow fiber contactors was investigated. The results clearly underline that the overall mass transfer coefficient of thallium depends on the aqueous phase flow rate and the module length. The major mass-transfer resistance is in the aqueous phase; the mass-transfer resistance in the organic phase outside the fibers and in the membrane pores is negligible. Both LTU and \bar{J} increase with increasing the aqueous flow rate, Q_w . LTU is higher for longer modules, but the thallium flux is higher for shorter modules. We observed that the type of hollow fiber polymer used for module fabrication (PP and PVDF) has no influence on the extraction of thallium. The laboratory-scale results presented suggest that hollow fiber contactors can be effectively used in pilot-plant installations for the production of radiopharmaceutical $^{201}\text{TlCl}$.

SYMBOLS

| | |
|-----------------|--|
| A | interfacial contact area, $\pi d_i NL \text{ (m}^2)$ |
| C | concentration of Tl(III) ($\text{kmol}\cdot\text{m}^{-3}$) |
| ΔC_{lm} | log mean concentration driving force in aqueous phase ($\text{kmol}\cdot\text{m}^{-3}$) |
| D | diffusivity of HTlCl_4 in aqueous phase ($\text{m}^2\cdot\text{s}^{-1}$) |
| D_o | diffusivity of HTlCl_4 in organic phase ($\text{m}^2\cdot\text{s}^{-1}$) |
| d_i | inner diameter of a hollow fiber (m) |
| d_o | outer diameter of a hollow fiber (m) |
| d_m | log mean diameter of a hollow fiber, $(d_o - d_i)/\ln(d_o/d_i)$ (m) |
| E | fraction of Tl(III) extracted (—) |
| Gr | Graetz number (—) |
| \bar{J} | mean flux of Tl(III) through interfacial area ($\text{kmol}\cdot\text{m}^{-2}\cdot\text{s}^{-1}$) |
| J | local flux of Tl(III) through interfacial area ($\text{kmol}\cdot\text{m}^{-2}\cdot\text{s}^{-1}$) |
| K_w | overall mass transfer coefficient based on aqueous phase ($\text{m}\cdot\text{s}^{-1}$) |
| k_{mo} | membrane mass transfer coefficient for hydrophobic membrane ($\text{m}\cdot\text{s}^{-1}$) |
| k_o | organic phase mass transfer coefficient ($\text{m}\cdot\text{s}^{-1}$) |
| k_w | aqueous phase mass transfer coefficient ($\text{m}\cdot\text{s}^{-1}$) |
| L | effective length of a hollow fiber (m) |



| | |
|---------------|---|
| LTU | length of transfer unit (m) |
| m_i | distribution coefficient of Tl(III) between organic and aqueous phases, C_o/C_w |
| NTU | number of transfer units (—) |
| N | number of hollow fibers in a module |
| Q_w | aqueous flow rate ($m^3 \cdot s^{-1}$) |
| Q_o | organic flow rate ($m^3 \cdot s^{-1}$) |
| Re | Reynolds number (—) |
| Sc | Schmidt number (—) |
| Sh | Sherwood number (—) |
| PP | polypropylene |
| PVDF | polyvinylidene fluoride |
| δ | thickness of membrane (m) |
| ε | porosity of membrane (—) |
| ν | kinematic viscosity of aqueous phase ($m^2 \cdot s^{-1}$) |
| τ | tortuosity of membrane (—) |

Subscripts and Superscripts

| | |
|-----|------------------------------------|
| in | inlet value of C |
| out | outlet value of C |
| o | C value in bulk of organic phase |
| w | C value in bulk of aqueous phase |
| ' | unsteady-state C value |

ACKNOWLEDGMENTS

The authors are indebted to Mr. B. Radojčić, R. Spajić, and B. Baškot, Department of Nuclear Medicine, Military Academy Hospital, Belgrade, for the grant of $^{201}\text{TlCl}$ samples.

REFERENCES

1. D. J. Pennal, R. Underwood, D. C. Costa, and P. J. Ell, *Thallium Myocardial Perfusion Tomography in Clinical Cardiology*, Springer-Verlag, London, 1992.
2. J. Singh Soin and H. L. Brooks (Eds.), *Nuclear Cardiology for Clinicians*, Futura Publishing, Mount Kisco, NY, 1980.
3. R. D. Neirinckx, *Radiochem. Radioanal. Lett.*, 5, 201 (1970).
4. T. V. Toribara and L. Koval, *Int. J. Appl. Radiat. Isot.* 29, 196 (1978).
5. S. M. Qaim, R. Weinreich, and H. Ollig, *Ibid.*, 30, 85 (1979).
6. N. Ramamoorthy and I. A. Watson, *Radiochem. Radioanal. Lett.*, 39, 309 (1979).
7. S. Bajo and A. Wytenbach, *J. Radioanal. Chem.*, 60, 173 (1980).
8. M. Bonardi, *Radiochem. Radioanal. Lett.*, 42, 35 (1980).
9. M. C. Lagunas-Solar, F. E. Little, and Ch.D. Goodart, *Int. J. Appl. Radiat. Isot.*, 33, 1439 (1982).



10. G. P. Kayfuss, T. E. Boothe, J. A. Campbell, R. D. Finn, and A. J. Gilson, *J. Radioanal. Chem.*, **68**, 269 (1982).
11. V. J. Sodd, K. L. Scholz, and J. W. Blue, *Ibid.*, **68**, 277 (1982).
12. A. B. Malinin, M. D. Kozlova, A. S. Sevastyanova, V. T. Kharlamov, G. P. Chursin, V. L. Kochetkov, V. T. Gladun, G. N. Chumikov, N. N. Krasnov, N. A. Konyakhin, V. M. Kulygin, and M. A. Abdukayumov, *Int. J. Appl. Radiat. Isot.*, **35**, 685 (1984).
13. M. D. Kozlova, A. B. Malinin, A. S. Sevastyanova, N. V. Kurenkov, N. I. Venikov, V. A. Shabrov, N. N. Krasnov, and N. A. Konyakhin, *Int. J. Radiat. Appl. Instrum. Part A, Appl. Radiat. Isot.*, **38**, 1090 (1987).
14. N. G. Zaitseva, C. Deptula, Kim Sen Khan, O. Knotek, P. Mikec, and V. A. Khalkin, *J. Radioanal. Nucl. Chem., Art.*, **121**, 307 (1988).
15. C. Deptula, N. G. Zaitseva, S. Mikolayewsky, and V. A. Khalkin, *Isotopenpraxis*, **26**, 476 (1990).
16. N. G. Zaitseva, C. Deptula, K. S. Khan, K. K. Khwan, S. Mikolaewsky, and V. A. Khalkin, *J. Radioanal. Nucl. Chem., Art.*, **149**, 235 (1991).
17. T. M. Trtić and J. J. Čomor, *Sep. Sci. Technol.*, **34**, 771 (1999).
18. W. S. Winston and K. K. Sirkar (Eds.), *Membrane Handbook*, Van Nostrand Reinhold, New York, NY, 1992.
19. J. G. Crespo and K. W. Böddeker (Eds.), *Membrane Processes in Separation and Purification*, Kluwer Academic Publishers, Dordrecht, 1993.
20. Y. Osada and T. Nakagawa (Eds.), *Membrane Science and Technology*, Dekker, New York, NY, 1992.
21. R. Basu, R. Prasad and K. K. Sirkar, *AIChE J.*, **36**, 450 (1990).
22. R. Prasad and K. K. Sirkar, *Sep. Sci. Technol.*, **22**, 619 (1987).
23. A. F. Seibert, X. Py, M. Mshewa, and J.R. Fair, *Sep. Sci. Technol.*, **28**, 343 (1993).
24. D. O. Cooney and C. C. Jackson, *Chem. Eng. Commun.*, **79**, 153 (1989).
25. R. Prasad and K. K. Sirkar, *AIChE J.*, **34**, 177 (1988).
26. L. Giorno, P. Spicka, and E. Drioli, *Sep. Sci. Technol.*, **31**, 2159 (1996).
27. B. M. Kim, *J. Membr. Sci.*, **21**, 5 (1984).
28. A. K. Guha, C. H. Yun, R. Basu, and K. K. Sirkar, *AIChE J.*, **40**, 1223 (1994).
29. R. Basu and K. K. Sirkar, *J. Membr. Sci.*, **75**, 131 (1992).
30. R. Basu and K. K. Sirkar, *AIChE J.*, **37**, 383 (1991).
31. M. A. Lévéque, *Ann. Mines Rec. Mem. L'Explotas Mines*, **13**, 201 (1928).
32. E. N. Sieder and G. E. Tate, *Ind. Eng. Chem.*, **28**, 429 (1936).
33. L. Dahuron and E. L. Cussler, *AIChE J.*, **34**, 130 (1988).
34. M. C. Porter, *Ind. Eng. Chem., Prod. Res. Dev.*, **11**, 234 (1972).
35. C. R. Wilke and P. Chang, *AIChE J.*, **1**, 264, (1955).
36. M. C. Yang and E. L. Cussler, *Ibid.*, **32**, 1910, (1986).
37. R. Prasad and K. K. Sirkar, *J. Membr. Sci.*, **50**, 153 (1990).
38. H. Gröber, S. Erk, and V. Grifull, *Fundamentals of Heat Transfer*, McGraw-Hill, New York, NY, 1961, p. 233.
39. R. Prasad, S. Khare, A. Sengupta, and K. K. Sirkar, *AIChE J.*, **36**, 1592 (1990).
40. N. A. D'Elia, L. Dahuron, and E. L. Cussler, *J. Membr. Sci.*, **29**, 309 (1986).
41. A. F. Seibert and J. R. Fair, *Sep. Sci. Technol.*, **32**, 573 (1997).
42. M. Knutsson, G. Nilvé, L. Mathiasson, and J. A. Jönsson, *J. Chromatogr. A*, **754**, 197 (1996).
43. J. T. F. Keurentjes, L. J. W. M. Nabuurs, and E. A. Vegter, *J. Membr. Sci.*, **113**, 351 (1996).

Received by editor August 30, 1999
 Revision received November 1999



Request Permission or Order Reprints Instantly!

Interested in copying and sharing this article? In most cases, U.S. Copyright Law requires that you get permission from the article's rightsholder before using copyrighted content.

All information and materials found in this article, including but not limited to text, trademarks, patents, logos, graphics and images (the "Materials"), are the copyrighted works and other forms of intellectual property of Marcel Dekker, Inc., or its licensors. All rights not expressly granted are reserved.

Get permission to lawfully reproduce and distribute the Materials or order reprints quickly and painlessly. Simply click on the "Request Permission/Reprints Here" link below and follow the instructions. Visit the [U.S. Copyright Office](#) for information on Fair Use limitations of U.S. copyright law. Please refer to The Association of American Publishers' (AAP) website for guidelines on [Fair Use in the Classroom](#).

The Materials are for your personal use only and cannot be reformatted, reposted, resold or distributed by electronic means or otherwise without permission from Marcel Dekker, Inc. Marcel Dekker, Inc. grants you the limited right to display the Materials only on your personal computer or personal wireless device, and to copy and download single copies of such Materials provided that any copyright, trademark or other notice appearing on such Materials is also retained by, displayed, copied or downloaded as part of the Materials and is not removed or obscured, and provided you do not edit, modify, alter or enhance the Materials. Please refer to our [Website User Agreement](#) for more details.

Order now!

Reprints of this article can also be ordered at
<http://www.dekker.com/servlet/product/DOI/101081SS100100242>